Original Article

High-dose vitamin C alleviates pancreatic injury via the NRF2/NQO1/HO-1 pathway in a rat model of severe acute pancreatitis

Li-Li Xu[#], Bing Zhao[#], Si-Lei Sun, Si-Fei Yu, Yu-Ming Wang, Ran Ji, Zhi-Tao Yang, Li Ma, Yi Yao, Ying Chen, Hui-Qiu Sheng, Er-Zhen Chen, En-Qiang Mao

Department of Emergency in Ruijin Hospital Affiliated to Shanghai Jiao Tong University School of Medicine, Shanghai, China

Contributions: (I) Conception and design: EQ Mao, Y Chen, B Zhao, LL Xu; (II) Administrative support: EZ Chen, EQ Mao, HQ Sheng; (III) Provision of study materials or patients: LL Xu , B Zhao, SL Sun, SF Yu; (IV) Collection and assembly of data: LL Xu , YM Wang, R Ji; (V) Data analysis and interpretation: B Zhao, ZT Yang, L Ma, Y Yao; (VI) Manuscript writing: All authors; (VII) Final approval of manuscript: All authors.

[#]These authors contributed equally to this work.

Correspondence to: En-Qiang Mao; Ying Chen. Ruijin 2# Road No. 197, Shanghai, China. Email: maoeq@yeah.net; bichatlion@163.com.

Background: Oxidative stress plays a pivotal role in the progress of severe acute pancreatitis (SAP). Vitamin C (VC) is the most important antioxidant in plasma. However, the effects of an intravenous administration of high-dose VC and the mechanisms by which it exerts its antioxidant function in an experimental model of SAP have not been determined.

Methods: Sodium taurocholate was used to induce rat pancreatic injury and AR42J cells injury. After the establishment of SAP model, SAP rat and injured AR42J cells were treated with VC. For the injured AR42J cells, small interfering RNA-mediated knockdown of NRF2 was conducted after VC treatment. The histopathological characteristics, the apoptosis of pancreatic acinar cells, oxidative stress markers and levels of enzymes, biochemical indicators, and inflammatory cytokines were examined *in vivo* and *in vitro*. Furthermore, the mortality of rats was assessed.

Results: *In vivo* and *in vitro* results demonstrated that VC treatment ameliorated apoptosis of pancreatic acinar cells, as evidenced by the increase in Bcl-2, Bcl-XL, and MCL-1 expressions and decrease in Bax and cleaved caspase-3 expression along with decreased TUNEL-positive cells. Also, we found that the elevation of MDA and decrease of SOD, GPx, GSH/GSSG, and T-AOC induced by SAP were reversed by VC treatment *in vivo* and *in vitro*, and VC treatment increased expressions of Nrf2, NQO1, and HO-1 in SAP model at protein and gene level, indicating that VC attenuated oxidative stress via the NRF2/NQO1/HO-1 pathway. Meanwhile, it was found that sodium taurocholate significantly induced the release of amylase, lipase, IL-1β, and IL-6 in rat plasma and AR42J cells, which were declined by VC treatment. *In vitro* results also revealed that these alterations in sodium taurocholate-injured AR42J cells due to VC treatment was attenuated by NRF2 knockdown. In addition, VC at a dose of 500 mg/kg decreased the levels of lactic acid, Cre, NGAL, AST, and ALT in the plasma of SAP rats, suggesting the improvement of renal and pancreatic injury and liver function of SAP rats. Furthermore, the mortality of SAP rats was 50%, which declined to 30% after VC treatment.

Conclusions: The present study suggests that high-dose of VC ameliorate pancreatic injury of SAP via the NRF2/NQO1/HO-1 pathway to inhibit oxidative stress.

Keywords: Severe acute pancreatitis (SAP); pancreatic acinar cells injury; vitamin C; oxidative stress; NRF2/NQO1/HO-1 pathway; inflammation

Submitted Dec 22, 2019. Accepted for publication Jun 21, 2020.

doi: 10.21037/atm-19-4552

View this article at: http://dx.doi.org/10.21037/atm-19-4552

Introduction

Severe acute pancreatitis (SAP) is defined as a persistent organ failure lasting more than 48 hours (1). Although treatment for this disease is improving, disease-related mortality is still reported to be as high as 30–40% (2,3). The pathogenesis of SAP has been the focus of many studies. At present, oxidative stress, excessive release of proinflammatory cytokines, overload of calcium, and dysregulated autophagy are considered the major mechanisms causing disease pathology (4-6). Particularly, oxidative stress caused by reactive oxygen species (ROS) plays a pivotal role in the progress of SAP (7,8), and thus, treatment with antioxidants may provide a good alternative therapy.

In the early phases of SAP, injured pancreatic acinar cells and activated immune cells in the pancreatic tissue release large amounts of ROS and reduce the capacity of the endogenous antioxidant defense system, which results in the accumulation of ROS and decrease of antioxidant enzymes like superoxide dismutase (SOD), glutathione peroxidase (GPx), quinone oxidoreductase1 (NQO1), and heme oxidase-1 (HO-1). Several studies performed in animal models of SAP showed that treatment with antioxidants had a protective effect in pancreatic tissue injury by modulating the nuclear factor erythroid-2 (NRF2) signaling pathway (7,9,10).

The NRF2 transcription factor is central for the cellular response to ROS and oxidative stress. Research has showed that NRF2 activity can improve cellular fitness under stress (11). Under basal conditions, cytosolic KEAP1 functions as an adapter for the E3 ubiquitin ligase Cullin-3 (CUL3) and constitutively targets NRF2 for ubiquitylation and degradation via the ubiquitin proteasome system. Upon exposure to oxidative stress, reactive cysteine residues in the KEAP1 structure prevent the degradation of NRF2. The stabilized NRF2 then translocates to the nucleus and binds to antioxidant-response elements (ARE) to regulate the expression of a set of antioxidant enzyme genes such as NQO1 and HO-1 (12,13). Previous studies have shown that the expression of NRF2 significantly decreased in the pancreatic tissues of mice with acute pancreatitis, and confirmed the protective effects of modulating the expression of NRF2 (7,9).

Vitamin C (VC) is the most important fast acting antioxidant in plasma, detoxifying exogenous oxidants' radical species as a first-line "ROS sink", while sparing other endogenous antioxidants (14). Low plasma concentrations of VC are associated with the severity of organ failure and mortality and previous studies have shown that critically ill patients have low plasma levels of VC (15,16), and that supplementing with VC improved their condition in diseases such as acute pancreatitis, sepsis, and hemorrhagic shock (16-18). No adverse effects of intravenous VC were registered in those studies. Our previous studies have shown that VC attenuates hemorrhagic shock-related multi-organ injuries through the induction of HO-1 (19) as well as may attenuate hemorrhagic shock-related renal injury via the SIRT1-NRF2-HO-1 pathway (18). To the best of our knowledge, there are few studies about the relationship between VC and NRF2.

In this study, we aim to investigate the protective effects and the potential mechanisms of a high dose of VC against sodium taurocholate-induced pancreatic acinar cells injury *in vitro* and *in vivo*. We present the following article in accordance with the ARRIVE reporting checklist (available at http://dx.doi.org/10.21037/atm-19-4552).

Methods

Animals

Sprague-Dawley (SD) rats (male, 8–10 weeks, 342.6±14.2 g) were used in this study. Animals were purchased from the Shanghai Laboratory Animal Center of the Chinese Academy of Science. All rats were kept on a 12 h light/dark cycle and fed with standard rat chow and tap water ad libitum. Before surgery, rats were fasted overnight with free access to water. Experiments were performed under a project license {No: SYXK[SHANG HAI] 2018-0027} granted by institutional of Animal Care and Use Committee, in compliance with Chinese guidelines for the care and use of animals.

SAP model

Surgical procedures were conducted under anesthesia with 2% isoflurane. SAP was induced as previously described (20). Retrograde infusion of a 5% sodium taurocholate solution (Sigma, St. Louis, MO, USA) (1 mL/kg) was performed into the biliopancreatic duct, at a constant rate of 3 mL/h. After completing the infusion, the part of the duct that enters the duodenum was clipped for 5 minutes. Next, the clip was removed and the wounds sutured. In the sham group, only an abdominal incision and sutures were made.

Animal experimental design

In the first stage, rats were randomly divided into five groups (n=6 in each group) to choose the optimal dose of VC: the sham surgery (SHAM), SAP, SAP + 100 mg/kg VC, SAP + 500 mg/kg VC, SAP + 1,000 mg/kg VC. After screening out the optimal dose of VC, rats were randomly divided into four groups (n=6 in each group) in the second stage: SHAM, SHAM + VC (optimal dose), SAP, SAP + VC (optimal dose). VC were injected into the tail vein of the rats after the establishment of SAP model. The SAP group rats received same volume of saline as a control.

All rats were sacrificed after 24 h and blood and pancreatic tissue were collected for further analysis. Blood samples were centrifuged at 3,000 rpm for 10 minutes to separate the serum and stored at −80 ℃ until analysis. A section of each pancreatic tissue sample was immediately fixed with 4% paraformaldehyde for HE staining and immunohistochemistry analysis. The remaining samples were stored at −80 ℃ for quantitative western blot and PCR analysis.

The following supplementary groups were also evaluated for mortality within 72 h: SAP group (n=10) and SAP + VC group (n=10).

Cell culture

AR42J rat pancreatic acinar cells (ATCC CRL-1492™), purchased from ATCC, were cultured in F-12K medium (SIGMA, USA) and supplemented with 20% fetal bovine serum and 1% antibiotic (containing 100 units/mL penicillin, and 100 μg/mL streptomycin) in a humidified atmosphere of 5% CO2 at 37 ℃.

Cell viability assay

AR42J cells were cultured in 96-well plates at a density of 1×10^5 cells mL^{-1} for 24 h, followed by treatment with various concentrations of VC (120, 250, 500, 1,000, 1,500, 2,000 μM) for 24 h. Cells in the control group were cultured under normal conditions without vitamin C. The cell viability was measured using the Cell Counting Kit-8 (CCK8) viability assay.

siNRF2 screening and treatment

The specific silencing of the NRF2 gene expression in AR42J cells was achieved by the siRNA technique. Three siNRF2, namely si-1 (5' GGAUGAAGAGACCGGAGAATT '3 and 5' UUCUCCGGUCUUCAUCCAG '3), si-2 (5' GAGGAUGGGAAACCUUACUTT '3 and 5' AGUAAGGUUUCCCAUCCUCAT '3), and si-3 (5' CCGAGUUACAGUGUCUUAATT '3 and 5' UUAAGACACUGUAACUCGGGA '3), and non-specific negative-siRNA (scramble group, 5' UUCUCCGAACGUGUCACGUdTdT'3 and 5' ACGUGACACGUUCGGAGAAdTdT '3) were chemically synthesized (Invitrogen) and effectively screened. The AR42J cells at 50% confluence were transfected with 50 nM siRNA mixed with lipofectamine 2000 (Invitrogen, Carlsbad, CA, USA) for 24–48 h according to the manufacturer's instruction. The effective interfere sequence for NRF2 from three candidate sequences was screened by detecting the relative expression of NRF2 using real-time PCR.

Following the screening of effective interfere sequence for NRF2, the AR42J cells were randomly divided into five groups: control, control + VC, SAP, SAP + VC, SAP + VC + siNRF2. The cell in the control and control + VC group were cultured under normal conditions without vitamin C and with 1,500 μM VC, respectively. The cell in the SAP, SAP + VC, and SAP + VC + siNRF2 groups were all treated with 500 μM sodium taurocholate for 1 h to induce cell injury, followed by treatment with 1,500 μM VC and 1,500 μM VC + 50 nM siNRF2 for the latter two groups, respectively.

Western blot

Total protein was extracted from AR42J cells and pancreatic tissue using 0.5 mL of cold RIPA lysis buffer containing protease and phosphatase inhibitors. Thereafter, their protein concentrations were quantificated using the BCA (Beyotime Biotechnology, Shanghai, China) method. Protein samples (20 μg per sample) from AR42J cells and rat pancreas were subjected to 10% sodium dodecyl sulfate-polyacrylamide gel electrophoresis and transferred onto polyvinylidene fluoride membranes (Millipore, Temecula, CA, USA). After blocking with 5% nonfat dried milk for 1 h at room temperature, the membranes were incubated with appropriate primary antibodies against NRF2 (1:1,000, Abcam, Cambridge, UK), NQO1 (1:10,000, Abcam, Cambridge, UK), HO-1 (1:1,000, Abcam, Cambridge, UK), procaspase 3, cleaved Caspase3, Bax, BCL-2, BCL-xL, MCL-1 and GAPDH (1:10,000, Abcam, Cambridge, UK) overnight at 4 ℃. After proper washing, the membranes were incubated for 1 hour with HRP-conjugated secondary

antibodies. The blots were detected using Western HRP Substrate (West Grove, PA, USA), and the results were visualized using the Tanon 5500 Imaging System (Shanghai, China).

Immunohistochemistry

NRF2, NQO1, and HO-1 staining was performed according to the Histostain-PlusKits (Abcam, Cambridge, UK) guidelines. After blocking, pancreas tissue and AR42J cell sections were incubated with NRF2, NQO1, HO-1 antibodies.

Histological study

HE stained slides were analyzed under an optical microscope and scored blinded by two independent pathologists. All assessments were performed on six fields per section under 400× magnification. Pancreatic histopathology scoring was performed according to Van Laethem *et al.* (21). Briefly, edema was graded from 0 to 3 (0: absent; 1: focally increased between lobules; 2: diffusely increased between lobules; 3: acinar disrupted and separated). Inflammatory cell infiltration was graded from 0 to 3 [0: absent; 1: in ducts (around ductal margins); 2: in parenchyma, <50% of the lobules; 3: in parenchyma, >50% of the lobules]. Acinar necrosis was graded as 0–3 (0: absent; 1: periductal necrosis, <5%; 2: focal necrosis, 5–20%; 3: diffuse parenchymal necrosis, 20–50%).

TUNEL staining

TUNEL assay was performed to detect cell apoptosis. The AR42J cells and pancreatic tissues were stained using the In Situ Cell Death Detection kit (Roche Diagnostics GmbH) according to the manufacturer's instructions. Apoptotic cells in tissue sections and cultural cells were observed under a fluorescence microscope and images were acquired.

Analysis of biochemical indicators

Arterial blood samples were processed immediately after collection by centrifugation at 3,000 rpm for 10 minutes to obtain plasma. The plasma levels of amylase, lipase, SOD, ALT, AST, lactic acid, Cre, and NGAL were measured using commercial assay kits (Jiancheng Bioengineering Institute, Nanjing, China). As for AR42J cells, the levels of amylase and lipase in cell supernatant were also measured.

Enzyme-linked immunosorbent assay (ELISA)

Quantification of IL-6 and IL-1β in the AR42J cells supernatant and rat plasma was performed using an ELISA kit (R&D, Minneapolis, MN) according to the manufacturer's instructions.

Determination of malondialdehyde (MDA), SOD, GPx, GSH/GSSG and T-AOC

MDA, SOD, GPx, GSH/GSSG and T-AOC levels in the AR42J cells supernatant and homogenized pancreatic tissue were measured using commercial kits (Beyotime, Shanghai, China) according to the manufacturers' instructions.

Real-time PCR

Total RNA was extracted from AR42J cells and pancreatic tissue using TRIZOL reagent (Life Technologies, Carlsbad, CA, USA). Total RNA was analyzed for concentration and purity and reverse transcribed into cDNA using the Prime Script RT Master Mix (Takara, Kyoto, Japan) according to the manufacturer's instructions.

To measure the expressions of NRF2, NQO1, and HO-1, RT-PCR was performed using the Step One Plus Real-time PCR system (Applied Biosystems, Carlsbad, CA, USA) with the Fast Start Universal SYBR Green Master mix. β-Actin was used as an internal control. Specific primers for rat NRF2, NQO1, HO-1, and β-Actin were designed using Primer Premier 5 and checked using Oligo6. The primers were indicated as follows: NRF2, 5' GCAACTCCAGAAGGAACAGG '3 and 5' GGAATGTCTCTGCCAAAAGC '3; HO-1, 5' ATCGTGCTCGCATGAACACT '3 and 5' CCAACACTGCATTTACATGGC '3; NQO1, 5' ACTCGGAGAACTTTCAGTACC '3 and 5' TTGGAGCAAAGTAGAGTGGT '3; β-Actin, 5' GCGCTCGTCGTCGACAACGG '3 and 5' GTGTGGTGCCAAATCTTCTTC '3. Primers were synthesized by Sangon Biotech Co. Ltd. (Shanghai). The following formula was used to calculate the relative quantity of mRNA: ratio $=2^{-\Delta\Delta Ct}$.

Statistical analyses

Data are expressed as mean ± S.E.M. Statistical analysis was performed using ANOVA or unpaired Student's *t*-test, as appropriate. A P value of <0.05 was considered to

indicate statistical significance. Statistical calculations were performed using Graph Pad Prism 8.

Results

Effects of different dose of VC on pancreatic injury and apoptosis of pancreatic acinar cells in rats model of SAP

Pancreatic tissues from the SAP group showed mass edema and inflammation with necrosis when compared with the SHAM and SAP + VC groups (*Figure 1A*,*B*). When SAP rats were treated with 100, 500 and 1,000 mg/kg of VC, it was found reduced edema, inflammatory cell infiltration and pancreatic necrosis in rat pancreatic tissue, which 500 mg/kg VC exerted the most obvious improvement on pancreatic injury as evidence of histological scores (*Figure 1A*,*B*).Then the effect of different dose of VC on apoptosis of pancreatic acinar cells in rats pancreatic tissue were further assessed. As shown in *Figure 1C*, the proportion of cells undergoing apoptosis in SAP group was higher than that in SHAM group, and 100, 500, and 1,000 mg/kg of VC could significantly reduce the proportion of apoptotic cells, of which 500 mg/kg showed the pronounced effect. Additionally, the expression of apoptosis-related protein (Bcl-2, Bcl-XL, MCL-1, Bax, cleaved caspase-3, and procaspase 3) was detected, and the results demonstrated an increased expression of Bcl-2, Bcl-XL, and MCL-1 and decreased expression of Bax and cleaved caspase-3 in pancreatic tissue from SAP group when compared with SHAM group (*Figure 1D*). The alteration of apoptosis-related proteins in SAP rats markedly weakened after receiving different doses of VC, especially 500 mg/kg of VC (*Figure 1D*). However, the expression of procaspase 3 showed no significant changes among these five groups (*Figure 1D*). Based on the above results, 500 mg/kg VC was selected as the treatment concentration of *in vivo* model for further analysis.

High-dose VC treatment reduced ascites and ameliorated apoptosis of pancreatic acinar cells in SAP rats

As showed in *Figure 2A*, the volume of ascites in SAP + VC group was significantly higher than that in the SAP group, indicating the likelihood of VC to reduce ascites in SAP rats. Moreover, the significantly increased expression of Bax and cleaved caspase-3 and TUNEL-positive cells and decreased expression of Bcl-2, Bcl-XL, and MCL-1 in the pancreatic tissue of SAP rats were revealed when compared to those in the SHAM group, and these effects were obviously decreased by VC at a dose of 500 mg/kg (*Figure 2B*,*C*,*D*), implying that VC treatment significantly reduced sodium taurocholate-induced pancreatic cell apoptosis in SAP rats. In addition, sodium taurocholate-induced edema, inflammatory cell infiltration and pancreatic necrosis in rat pancreatic tissue was markedly reduced (*Figure 2E*).

High-dose VC attenuated oxidative stress via the NRF2/NQO1/HO-1 pathway in SAP rats

MDA, SOD, GPx, GSH/GSSG and T-AOC were analyzed in pancreas tissue homogenates as indicators of lipid peroxidation and activity of antioxidant enzymes. As showed in *Figure 3A*, induction of SAP was resulted in an elevation of MDA and decreasement of SOD, GPx, GSH/GSSG and T-AOC compared to the SHAM group. Following VC treatment, changes of these levels in SAP rats have been significantly reversed (*Figure 3A*), suggesting that VC at a dose of 500 mg/kg attenuated oxidative stress in SAP rats.

To determine whether the Nrf2/ARE pathway could contribute to the induction of antioxidant enzymes by VC, the mRNA level and protein expression of Nrf2 and ARE-mediated genes NQO1 and HO-1 were further analyzed. As shown in *Figure 3B*,*C*, the protein and mRNA expression of Nrf2, NQO1 and HO-1 as well as nuclear NRF2 protein expression in the SAP group was significantly lower than those in the SHAM group. In contrast, Nrf2, NQO1 and HO-1 protein and mRNA expression in the SAP + VC group was significantly higher than SAP group (*Figure 3B*,*D*). Increased expression of Nrf2, NQO1 and HO-1 by VC was also demonstrated by immunohistochemistry (*Figure 3E*). These results indicated that VC inhibited oxidative stress via the NRF2/NQO1/HO-1 pathway in SAP rats.

High-dose VC ameliorated biochemical indicators and attenuated the systemic inflammatory response in SAP rats

Amylase and lipase are hallmark parameters of pancreatitis. As shown in *Figure 4A*,*B*, amylase and lipase activity in plasma were significantly increased in the SAP group than in the SHAM group ($P<0.01$), indicating that the induction of SAP was successful. However, the levels of amylase and lipase both decreased in the SAP + VC group compared to the SAP group ($P<0.05$). Lactic acid, Cre and NGAL are measurable parameters of renal injury, and AST and ALT are biochemical markers of liver function. Our results

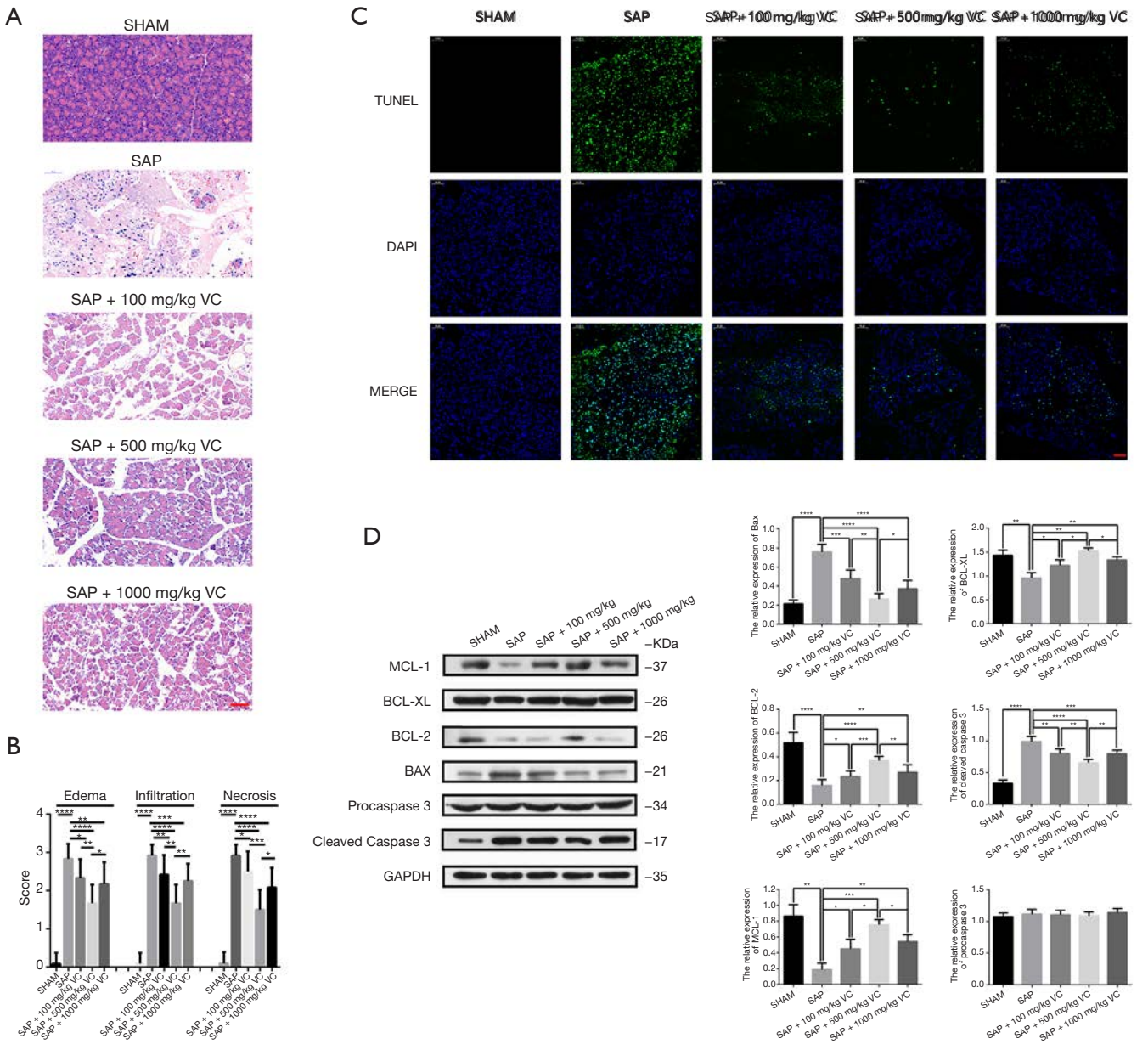

Figure 1 Effects of different dose of vitamin C (VC) on pancreatic injury and apoptosis of pancreatic acinar cells in rats model of severe acute pancreatitis (SAP). (A) HE sections in pancreatic tissues from rats of SAP and SAP treated with 100, 500 and 1,000 mg/kg VC group. (B) Histological score of pancreatic tissues in rats. (C) TUNEL immunostaining in pancreatic tissues of rats treated with or without 100/500 mg/kg VC after SAP. (D) Western blot analysis of BCL-2, Bcl-XL, MCL-1, Bax, cleaved caspase 3, and procaspase 3 in pancreatic tissues from rats of SAP and SAP treated with 100, 500, and 1,000 mg/kg VC groups. *, P<0.05; **, P<0.01; ***; P<0.001; ****, P<0.0001. P values were analyzed by ANOVA and unpaired Student's *t*-test. Scale bar represents 50 μm. SHAM, sham operation group; SAP, sodium taurocholate-induced severe acute pancreatitis group; SAP + 100 mg/kg VC group, SAP treated with 100 mg/kg VC; SAP + 500 mg/kg VC group, SAP treated with 500 mg/kg VC group; SAP + 1,000 mg/kg VC group, SAP treated with 1,000 mg/kg VC; HE, haematoxylin-eosin staining; TUNEL, terminal deoxynucleotidyl transferase-mediated dUTP-biotin nick end labeling assay.

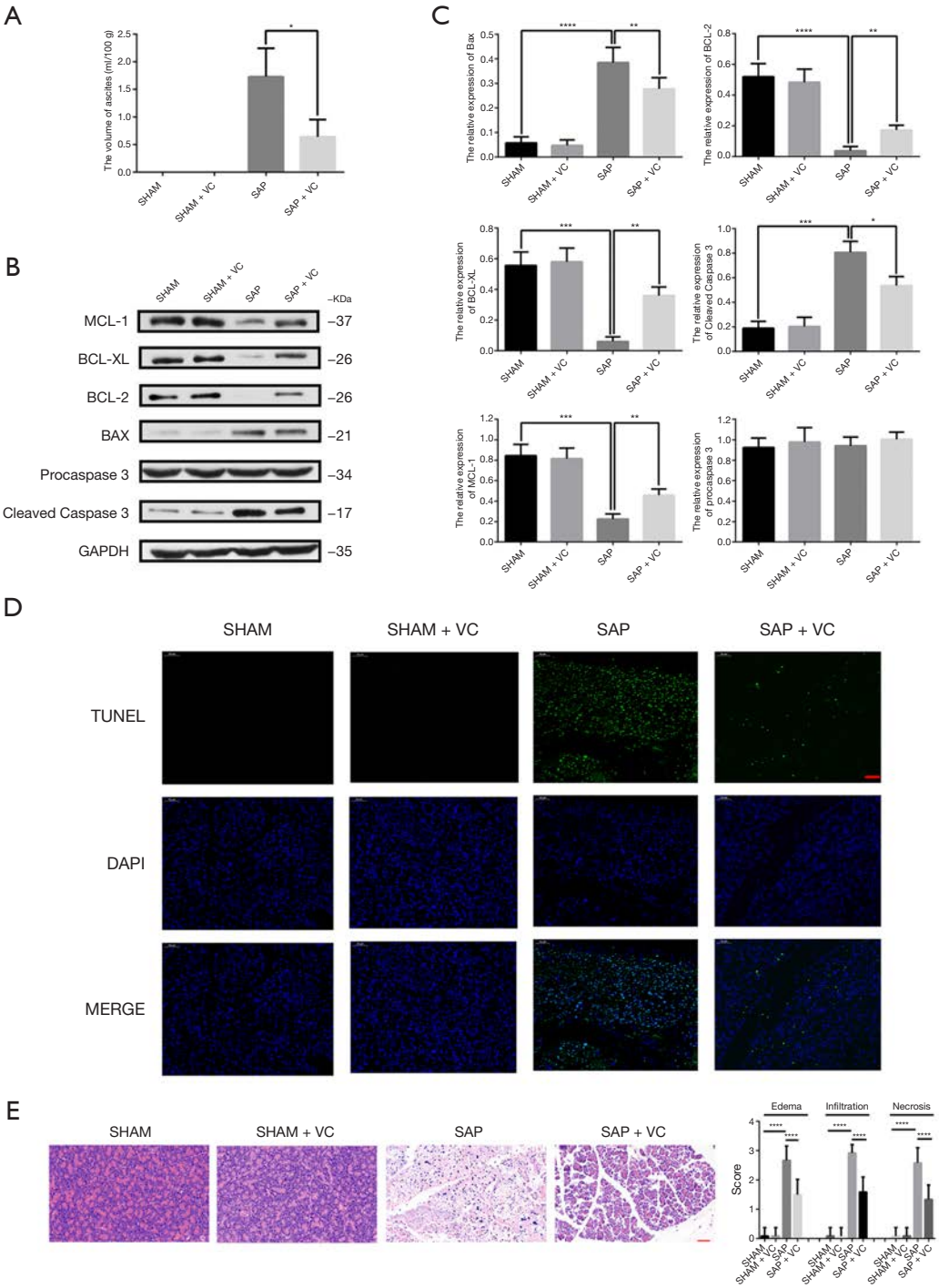

Figure 2 High-dose VC ameliorates pancreatic injury in SAP rats. (A) High-dose VC reduced ascites in SAP rats. (B,C) Western blot analysis of BCL-2, Bcl-XL, MCL-1, Bax, cleaved caspase 3 and procaspase 3 in pancreatic tissues from rats of SAP and SAP treated with 500 mg/kg VC. (D) TUNEL immunostaining in pancreatic tissues from rats of SAP and SAP treated with 500 mg/kg VC. (E) HE sections and Histological score of pancreatic tissues from rats of SAP and SAP treated with 500 mg/kg VC. *, P<0.05; **, P<0.01; ***, P<0.001; ****, P<0.0001. P values were analyzed by ANOVA and unpaired Student's *t*-test. Scale bar represents 50 μm. SHAM, sham operation group; SHAM + VC, sham operation treated with 500 mg/kg VC; SAP, sodium taurocholate induced severe acute pancreatitis group; SAP + VC, SAP treated with 500 mg/kg VC; TUNEL, terminal deoxynucleotidyl transferase-mediated dUTP-biotin nick end labeling assay.

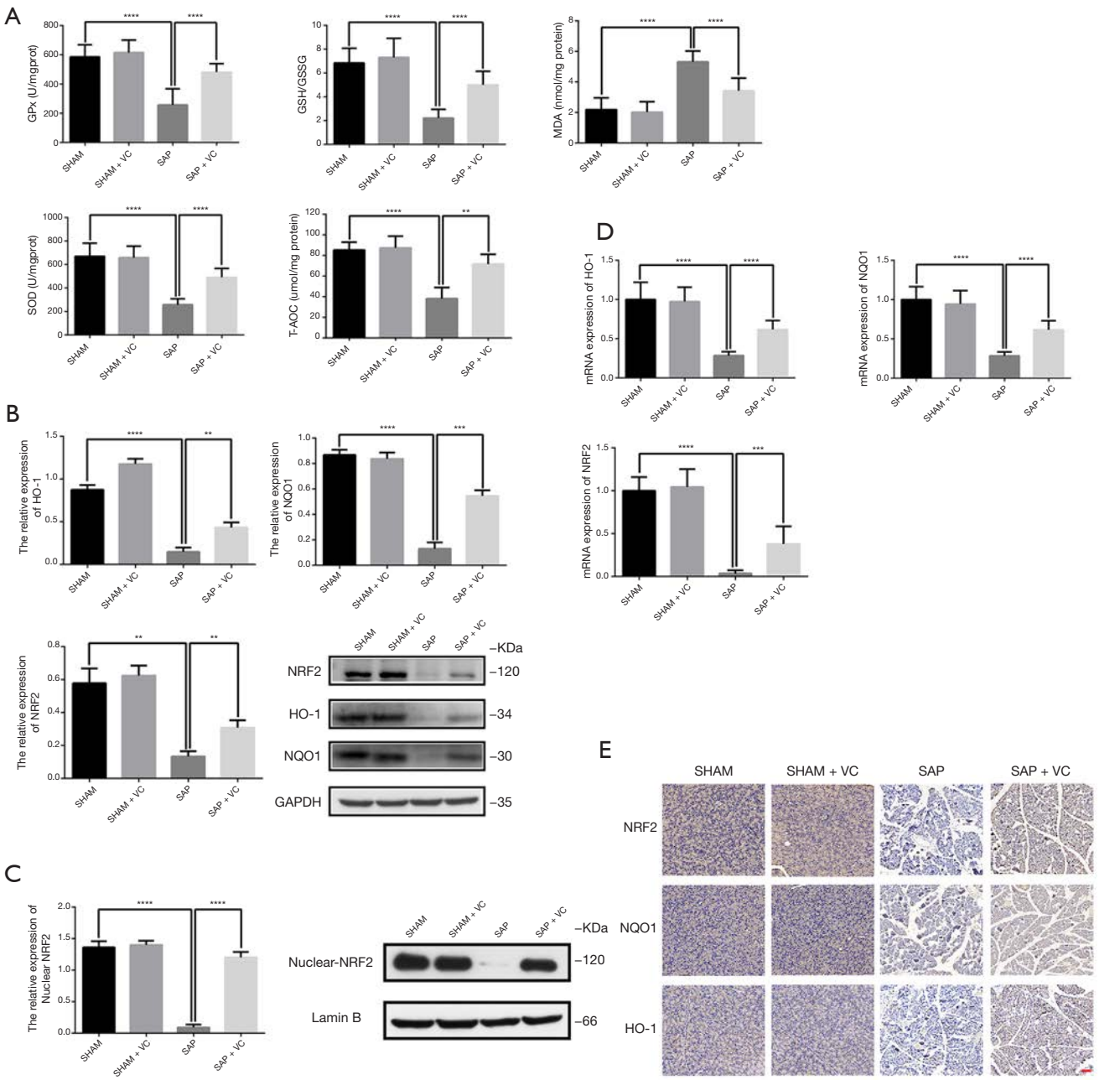

Figure 3 High-dose VC attenuates oxidative stress in SAP rats. (A) Pancreatic level of MDA, SOD, GPx, GSH/GSSG and T-AOC. (B) Western blot analysis of NRF2, HO-1, and NQO-1 in pancreatic tissue of rats. (C) Western blot analysis of nuclear NRF2 in pancreatic tissue of rats. (D) mRNA expression level of Nrf2, NQO-1, and HO-1 in pancreatic tissue of rats. (E) Immunohistochemical staining for Nrf2, NQO-1, and HO-1 in pancreatic tissue of rats. **, P<0.01; ***, P<0.001; and ****, P<0.0001. P values were analyzed by ANOVA and unpaired Student's *t*-test. Scale bar represents 50 μm. SHAM, sham operation group; SHAM + VC, sham operation treated with 500 mg/kg VC; SAP, sodium taurocholate induced severe acute pancreatitis group; SAP + VC, SAP treated with 500 mg/kg VC group; MDA, malondialdehyde; SOD, superoxide dismutase; GPx, glutathione peroxidase; GSH/GSSG, glutathione reduced/glutathione oxydized; T-AOC, total-anti-oxidizing-capability; NRF2, nuclear factor erythroid-2; NQO1, quinone oxidoreductase1; HO-1, heme oxidase-1.

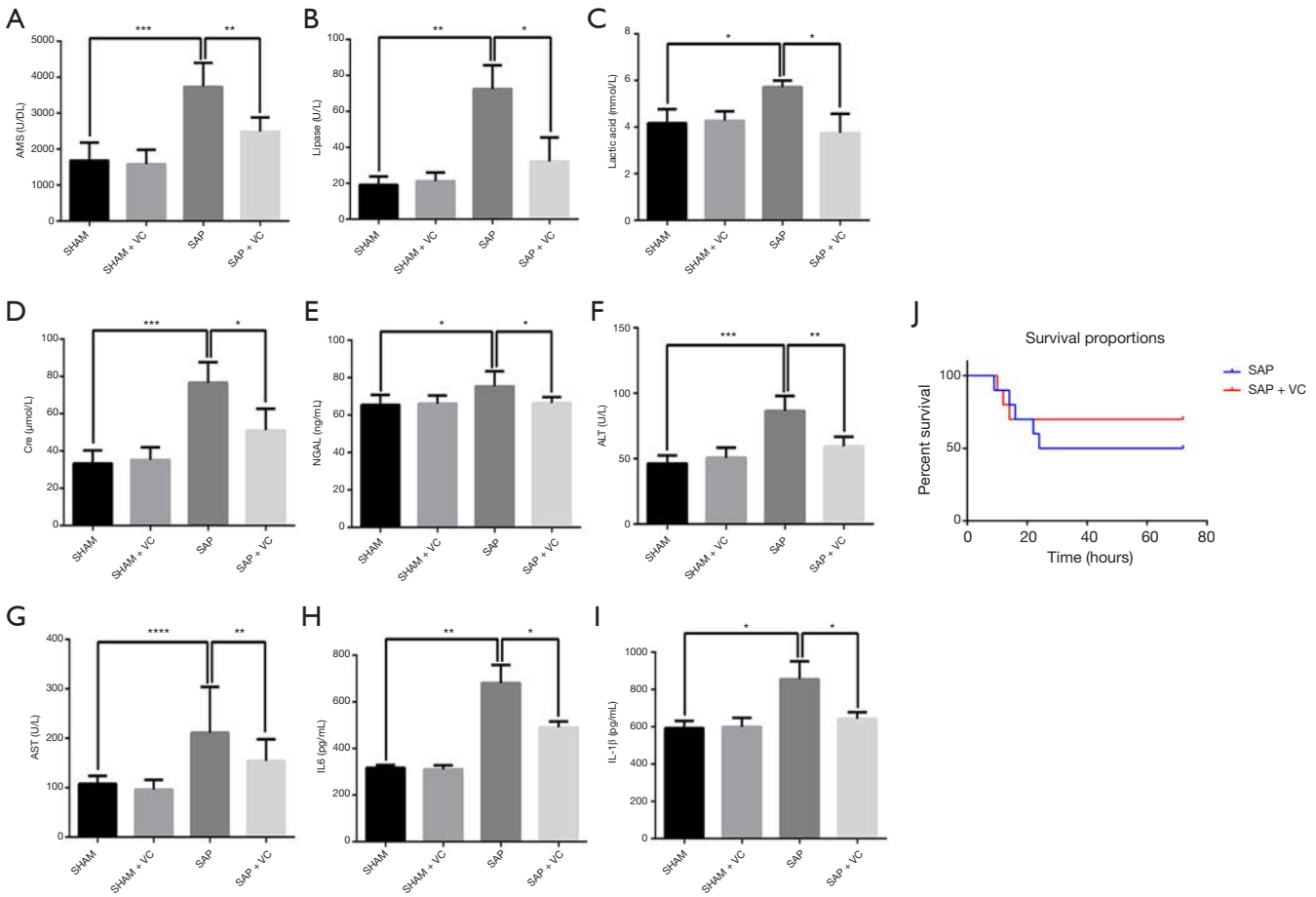

Figure 4 High-dose VC ameliorated biochemical indicators, systemic inflammatory response, and decreased the mortality of SAP rats. (A,B,C,D,E,F,G,H,I) Concentration of amylase, lipase, lactic acid, Cre, NGAL, AST, ALT IL-6 and IL-1β in the plasma of rats. (J) High-dose VC decreased the mortality of SAP rats. *, P<0.05; **; P<0.01; ***; P<0.001; ****, P<0.0001. P values were analyzed by ANOVA and unpaired Student's *t*-test. SHAM, sham operation group; SHAM + VC, sham operation treated with 500 mg/kg VC; SAP, sodium taurocholate induced severe acute pancreatitis group; SAP + VC, SAP treated with 500 mg/kg VC group; Cre, creatinine; NGAL, neutrophil gelatinase associated lipids carry proteins; AST, glutamic oxaloacetic transaminase; ALT, glutamic pyruvic transaminase.

showed that the levels of these indicators in plasma of SAP rat were all significantly decreased after treatment with VC (*Figure 4C,D,E,F,G*, P<0.05), indicating VC at a dose of 500 mg/kg may improve the injury of renal and pancreas and liver function of SAP rat.

IL-1β and IL-6 are important inflammatory factors involved in pancreatitis. Thus, the inflammatory cytokines (IL-1β and IL-6) in the rat plasma was measured. It was found a drastic increase in the levels of IL-1β and IL-6 in the plasma of the SAP group compared to the SHAM group (P<0.05 for both IL-1β and IL-6; *Figure 4H,I*). However, the levels of IL-1β and IL-6 in SAP rat were significantly reduced after receiving 500 mg/kg VC treatment, showing that VC attenuated the systemic inflammatory response in SAP rats.

High-dose VC decreased the mortality of SAP rats

As shown in *Figure 4J*, the mortality in the SAP group rats was 50%, whereas it was significantly reduced to 30% following VC (500 mg/kg) treatment (P<0.05), indicating that VC may decrease the mortality of SAP rats.

Effects of different concentrations of VC on AR42J cells

In order to choose the ideal concentration of VC for the *in vitro* model, the viability of AR42J cells treated with

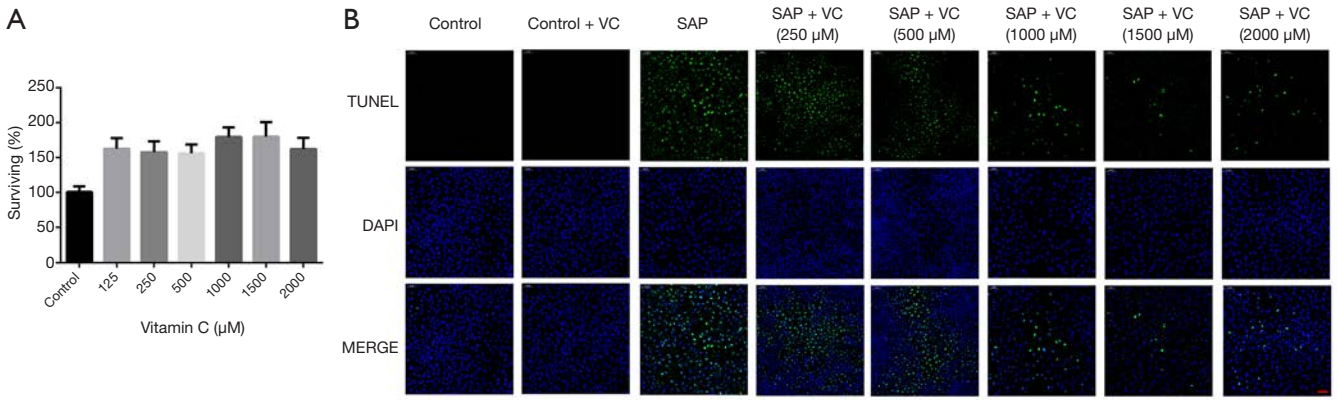

Figure 5 Effects of different concentrations of VC on AR42J cells. (A) Effects of different concentrations of VC (250, 500, 1,000, 1,500, 2,000 μM) on the viabilities of AR42J cells. (B) TUNEL immunostaining in AR42J cells treated without or with different concentrations of VC (250, 500, 1,000, 1,500, 2,000 μM). Scale bar represents 50 μm. TUNEL, terminal deoxynucleotidyl transferase-mediated dUTP-biotin nick end labeling assay.

different VC concentrations (250, 500, 1,000, 1,500, and 2,000 μM) was detected through a CCK8 assay, and the results illustrated that the activity and survival rates of AR42J cells did not decrease (*Figure 5A*), suggesting that VC in this concentration range of 250–2,000 μM has no toxic effect on normal pancreatic acinar cells. Additionally, the effect of different VC concentration on sodium taurocholate-induced apoptosis of AR42J cells was further evaluated via TUNEL staining. As shown in *Figure 5B*, a large number of apoptotic cells was observed in the SAP group. However, concentrations of 250, 500, 1,000, 1,500, and 2,000 μM of VC significantly reduced the proportion of apoptotic cells, suggesting that VC alleviates sodium taurocholate-induced AR42J apoptosis. Meanwhile, there was no significant difference when reducing apoptotic cells between 1,500 and 2,000 μM VC; 1,500 μM VC was selected as the treatment concentration for the *in vitro* model.

Knockdown of NRF2 attenuated the protective effects of VC on sodium taurocholate-induced AR42J cell injury

To further explore the role of NRF2 in the protective effects of VC, small interfering RNA (siRNA)-mediated knockdown of NRF2 in AR42J cell was carried out. Our data reported that the NRF2 siRNA sequences 1 (si-1) and 2 (si-2) significantly decreased NRF2 mRNA level compared with scramble group, but the NRF2 siRNA sequence 3 (si-3) had no obvious knockdown effect on NRF2 mRNA level (*Figure S1*). Hence, si-2 with the highest knockdown efficiency was selected for subsequent experiments.

Knockdown of NRF2 attenuated the inhibited effects of VC on sodium taurocholate-induced AR42J cell apoptosis

As shown in *Figure 6A*, the increased expressions of Bax and cleaved caspase-3 induced by sodium taurocholate were significantly reduced following treatment with VC. Conversely, the expression of Bcl-2, Bcl-XL, and MCL-1 markedly decreased after sodium taurocholate stimulation; however, the alteration was reversed by VC treatment (*Figure 6A*). These results suggested the VC reduced sodium taurocholate-induced apoptosis of AR42J cells, which similar results were also observed in a TUNEL assay (*Figure 6B*). However, these actions of VC on sodium taurocholate-injured AR42J were weaken by NRF2 knockdown (*Figure 6A,B*), implying the involvement of NRF2 in the underlying mechanism of VC against sodium taurocholate-induced AR42J cell apoptosis.

Knockdown of NRF2 weaken the effects of VC on sodium taurocholate-induced oxidative stress in AR42J cell

AR42J cell apoptosis linked to oxidative stress has been implicated in pancreatitis. Therefore, the effect of VC on oxidative stress in AR42J cells induced by sodium taurocholate was determined. As displayed in *Figure 7A,B,C*, the NRF2, HO-1, and NQO1 were markedly decreased in SAP group compared with control group, but they were notably increased in SAP + VC group at both gene and protein levels when compared with SAP group. Similar results were also confirmed by immunohistochemistry (*Figure 7D*).

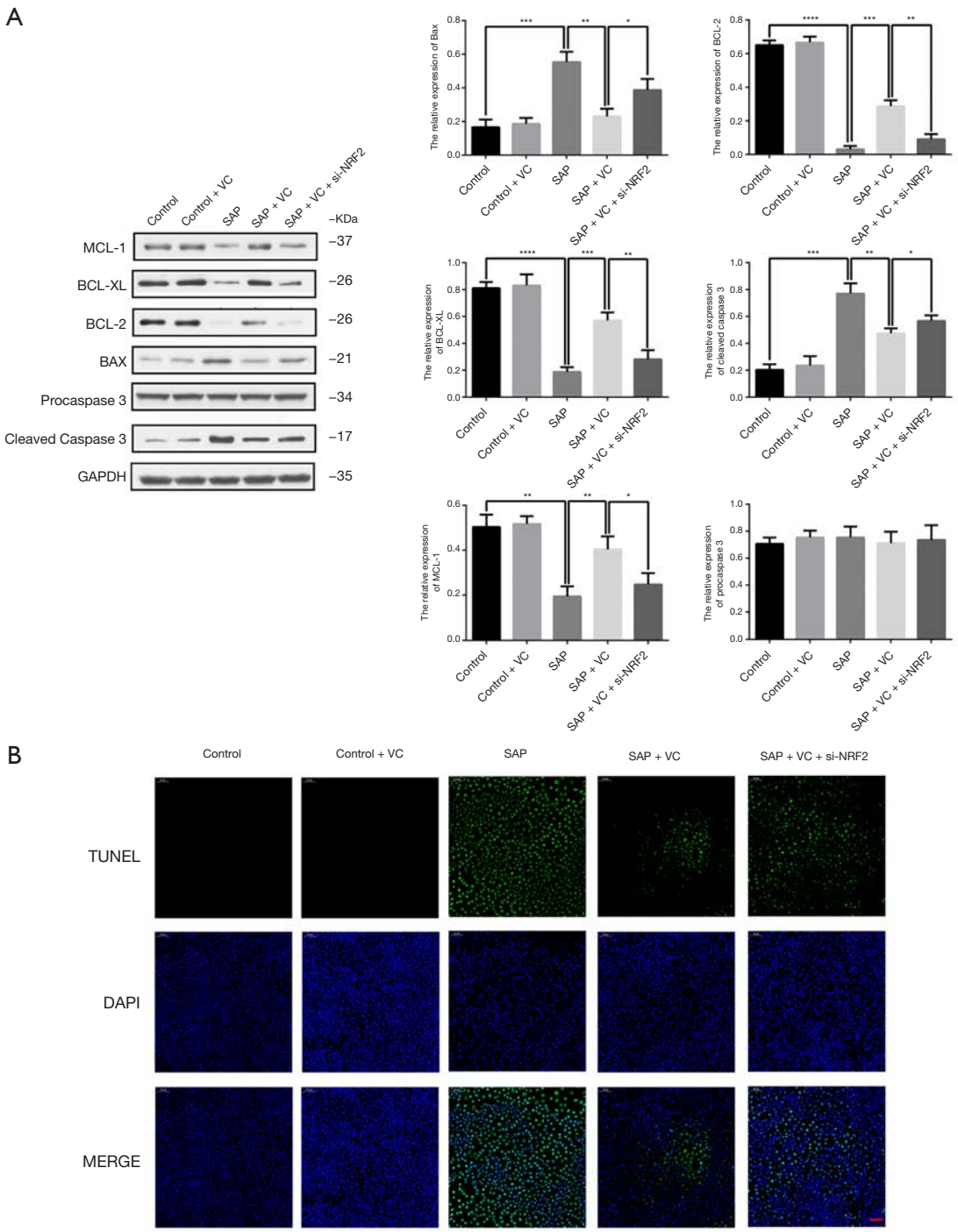

Figure 6 Knockdown of NRF2 attenuated the inhibited effects of VC on sodium taurocholate-induced AR42J cell apoptosis. (A) Western blot analysis of BCL-2, Bcl-XL, MCL-1, Bax, cleaved caspase 3, and procaspase 3 in AR42J cell. (B) TUNEL immunostaining in AR42J cell. *, P<0.05; **, P<0.01; ***, P<0.001; ****, P<0.0001. P values were analyzed by ANOVA and unpaired Student's *t*-test. Scale bar represents 50 μm. Control group, normal AR42J cell; control + VC group, normal AR42J cell treated with 1,500 μM VC; SAP group, AR42J cell treated with sodium taurocholate; SAP + VC group, sodium taurocholate-injured AR42J cell treated with 1,500 μM VC; SAP + VC + siNRF2, sodium taurocholate-injured AR42J cell treated with 1,500 μM VC and 50 nM siNRF2; NRF2, nuclear factor erythroid-2; TUNEL, terminal deoxynucleotidyl transferase-mediated dUTP-biotin nick end labeling assay.

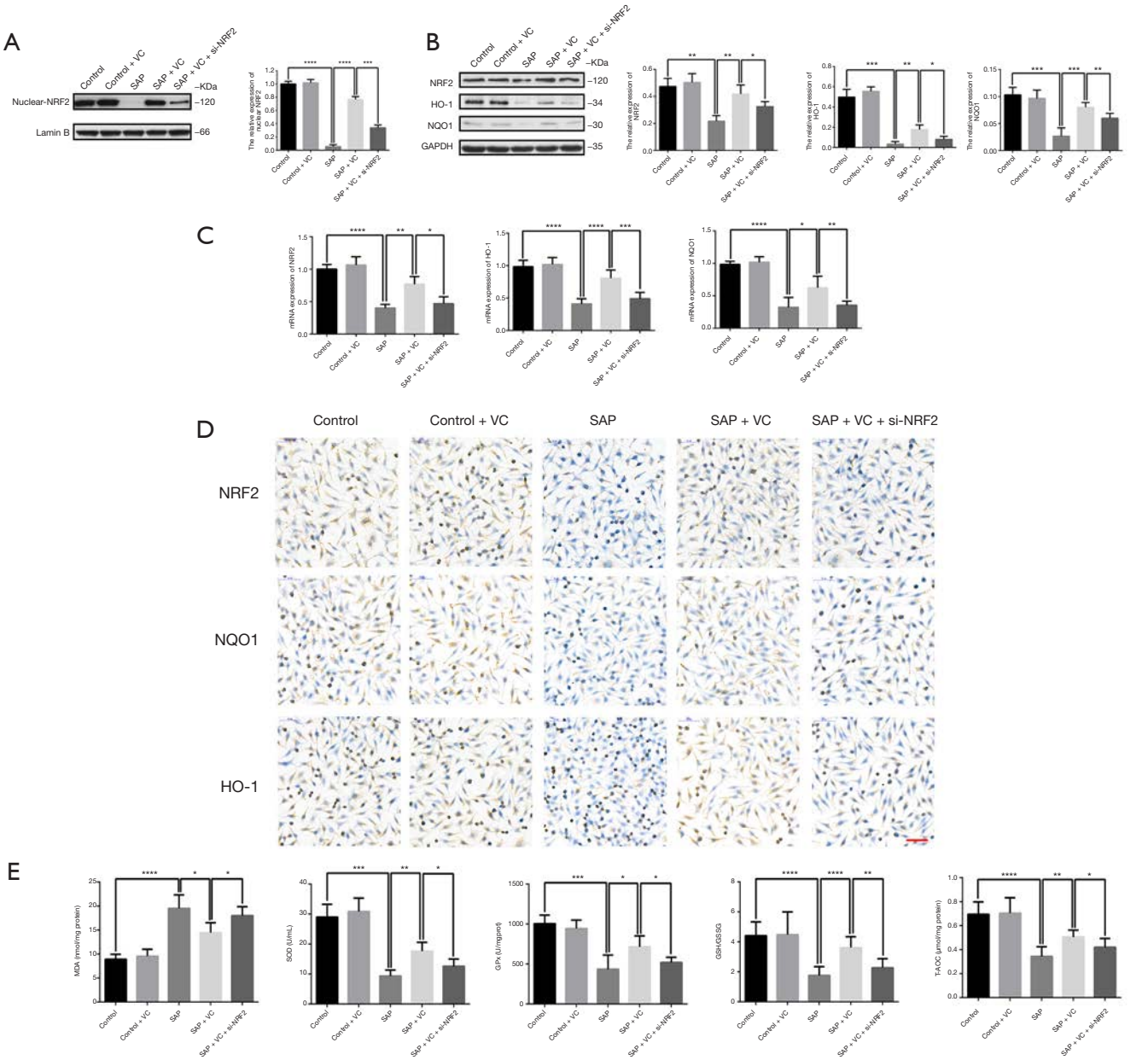

Figure 7 Knockdown of NRF2 weakens the effects of VC on sodium taurocholate-induced oxidative stress in AR42J cell. (A) Western blot analysis of nuclear NRF2. (B) Western blot analysis of NRF2, HO-1, and NQO-1 in AR42J cell. (C) mRNA expression level of Nrf2, NQO-1, and HO-1 in AR42J cell. (D) Immunohistochemical staining for Nrf2, NQO-1, and HO-1 in AR42J cell. (E) Levels of MDA, SOD, GPx, GSH/GSSG and T-AOC in the AR42J cell supernatant. *, P<0.05; **, P<0.01; ***, P<0.001; ****, P<0.0001. P values were analyzed by ANOVA and unpaired Student's *t*-test. Scale bar represents 50 μm. Control group, normal AR42J cell; control + VC group, normal AR42J cell treated with 1,500 μM VC; SAP group, AR42J cell treated with sodium taurocholate; SAP + VC group, sodium taurocholate-injured AR42J cell treated with 1,500 μM VC; SAP + VC + siNRF2, sodium taurocholate-injured AR42J cell treated with 1,500 μM VC and 50 nM siNRF2; NRF2, nuclear factor erythroid-2; NQO1, quinone oxidoreductase1; HO-1, heme oxidase-1; MDA, malondialdehyde; SOD, superoxide dismutase; GPx, glutathione peroxidase; GSH/GSSG, glutathione reduced/glutathione oxydized; T-AOC, total-anti-oxidizing-capability.

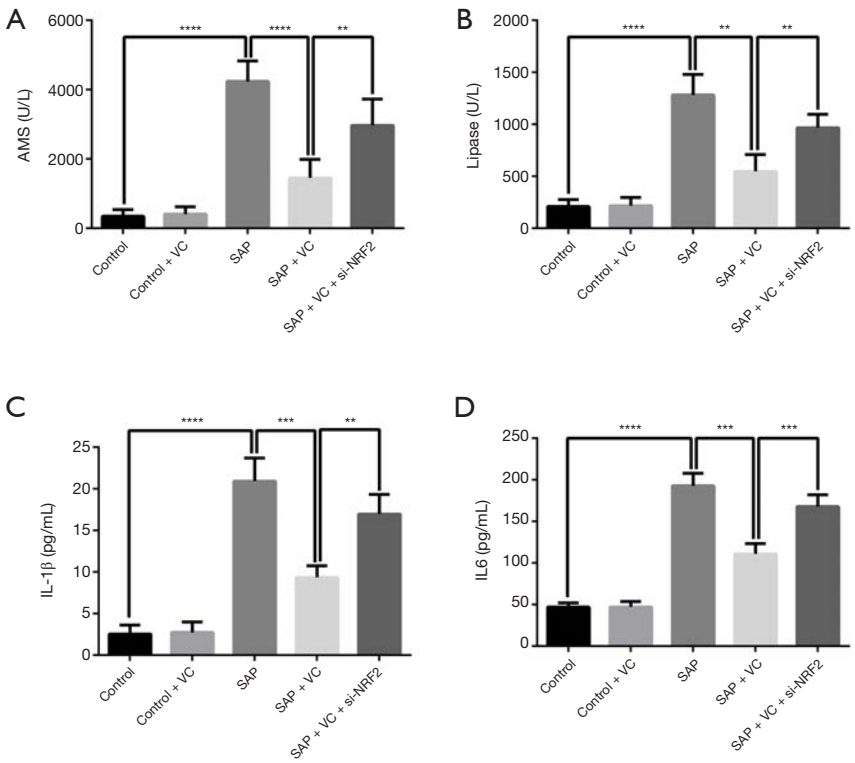

Figure 8 Knockdown of NRF2 attenuated the effects of VC on sodium taurocholate-induced release of amylase, lipase, IL-1β and IL-6 in AR42J cells. **, P<0.01; ***, P<0.001; ****, P<0.0001. P values were analyzed by ANOVA and unpaired Student's *t*-test. Control group, normal AR42J cell; control + VC group, normal AR42J cell treated with 1,500 μM VC; SAP group, AR42J cell treated with sodium taurocholate; SAP + VC group, sodium taurocholate-injured AR42J cell treated with 1,500 μM VC; SAP + VC + siNRF2, sodium taurocholate-injured AR42J cell treated with 1,500 μM VC and 50 nM siNRF2; NRF2, nuclear factor erythroid-2.

Meanwhile, the levels of MDA, SOD, GPx, GSH/GSSG, and T-AOC in cell culture supernatant were also detected, and the results showed markedly decreased levels of SOD, GPx, GSH/GSSG, and T-AOC and increased MDA level in SAP group when compared with control group (*Figure 7E*). After treated with VC, these changes of MDA, SOD, GPx, GSH/GSSG, and T-AOC in the SAP group were evidently reduced (*Figure 7E*). However, these alterations in sodium taurocholate injured AR42J cells caused by VC treatment was attenuated by NRF2 knockdown (*Figure 7A,B,C,D,E*).

Knockdown of NRF2 attenuated the effects of VC on sodium taurocholate-induced release of amylase, lipase, IL-1β and IL-6 in AR42J cells

Through ELISA, it was found that sodium taurocholate significantly induced the release of amylase, lipase, IL-1β, and IL-6 in AR42J cells, which was declined by VC treatment (*Figure 8*). Nevertheless, NRF2 knockdown undermined the effect of VC on the amylase, lipase, IL-1β, and IL-6 in sodium taurocholate-injured AR42J cells (*Figure 8*).

Discussion

The present study demonstrated that a high dose of VC could significantly alleviate SAP-related pancreatic damage, reduce the volume of ascites of SAP rats , decrease apoptosis of pancreatic acinar cells, attenuate oxidative stress in the pancreas by modulating the NRF2/NQO1/HO-1 pathway, decrease the levels of plasma biochemical indicators, ameliorate inflammatory insult, and could decrease the mortality of SAP rats.

Although the pathogenesis of SAP is not fully understood, research indicates that oxidative stress plays a key role (8). During SAP, the excessive production and accumulation of ROS leads to a decline of the intrinsic

antioxidative defense system. High amounts of ROS could attack the biomembrane and cause unsaturated fatty acid lipid peroxidation, destroy major enzymes, and disturb the synthesis and replication of DNA; whereas, lipid peroxidation could produce more toxic substances and free radicals (22).

As a water-soluble high abundance antioxidant and the most effective endogenous antioxidant, the benefits of high intravenous dose of vitamin C in critically ill patients have already been reported. Serum concentrations of VC were found to be lower in critically ill patients. Spoelstra-de Man *et al.* showed that a high intravenous dose of VC could increase its plasma concentration and subsequently yield more potent antioxidant effects in these patients (14,23). Du *et al.* demonstrated that following a high-dose administration of VC, patients with SAP took shorter time to improve their clinical symptoms and to normalize their serum levels of amylase and leukocyte counts than those receiving a lower dose of VC (16). Tanaka *et al.* demonstrated that patients with severe burn who were treated with a high dose of VC (110 g/d) required less fluid resuscitation and tended to have a reduced hospitalization stay and mortality (24). Although the doses of VC used in these studies varied, most found that a higher dose of VC proved to be more effective in critically ill patients.

The effective dose of VC used in experimental animal models of SAP has seldom been reported. Some animal studies that showed beneficial effects of VC in sepsis (25), ischemia reperfusion (26), and hypovolemic shock (19), have used 10–50 mg/kg as a low dose, and 100–200 mg/kg as a high dose. In these studies, the higher dose VC showed better effects in organ protection and in the improvement of survival. In our study, we demonstrated that VC at a dose of 500 mg/kg proved more effective in alleviating pancreatic injury in SAP rats than 100 mg/kg and 1,000 mg/kg). Moreover, we did not find that VC at a dose of 500 mg/kg caused kidney injury in the animals. Our results indicated that, on the contrary, VC could alleviate kidney and pancreas injury and improve liver function in our experimental model. In this study, the effect of 1,000 mg/kg VC has not been explored in detail, considering that rats may have side effects at this dose, such as kidney damage.

Furthermore, our results showed that intravenous VC decreased the mortality caused by SAP and significantly attenuated edema, inflammation, and necrosis in the pancreas tissues of SAP rats. We also found that VC significantly reduced ascites induced by SAP. In future, we will further explore the mechanism by which VC exerts these effects and investigate different administration routes and doses. Further research on VC may provide new insights into the development of therapies for ascites in SAP.

Previous research showed that VC could suppress tumor necrosis factor-α (TNF-α)-induced nuclear factor kappa-B (NF-κB) activation by inhibiting inhibitory kappa-B kinase (IκB kinase) phosphorylation (27). Similarly, our results showed that VC significantly reduced the levels of inflammatory cytokines (IL-1β and IL-6), which points to a role of VC as an anti-inflammatory.

A high dose of VC can directly scavenge superoxide, inhibit activation of nicotinamide adenine dinucleotide phosphate oxidase (NADPH-ox), and induce nitric oxide synthase. It can also prevent the uncoupling of oxidative phosphorylation, augment tetrahydrobiopterin (BH4), and reduce superoxide and peroxynitrite formation. All these events lead to a decrease in oxidative damage and mitigate organ dysfunction during sepsis and ischemia/reperfusion injury (28,29). Our previous studies showed that VC can attenuate hemorrhagic shock-related multi-organ injuries through the induction of HO-1 (19). It is possible that VC attenuates hemorrhagic shock-related renal injury via the SIRT1-NRF2-HO-1 pathway (18). To the best of our knowledge, there are few studies that have looked at the relationship between VC and NRF2.

Because NRF2 was shown to activate oxidative stress inducible genes, NRF2 inducers have been used in reperfusion injuries of the brain (30), heart (31), and kidney (32), neurodegenerative disorders, such as Alzheimer's disease, that have all been linked to oxidative stress (33), as well as in metabolic disorders, such as obesity (34) and diabetes (35,36), which are closely related to dysregulation of oxidative stress,. NRF2 inducers alleviated tissue damage following ischemia reperfusion, attenuated the neuronal symptoms of these diseases, and improved the control of systemic metabolism and obesity. Previous studies have shown that the expression of NRF2 was significantly decreased in the pancreatic tissues of mice models with acute pancreatitis and confirmed that the protective effects of NRF2 were observed upon modulation of its expression (7,9). Our results showed that the levels of NRF2 mRNA and protein were significantly decreased in SAP rats, but that VC treatment induced the activation of NRF2, enhanced its nuclear translocation, and subsequent ARE-binding in the NQO1 and HO-1 loci. We also unclosed that knockdown of NRF2 attenuates the protective effects of VC on sodium taurocholate-induced AR42J Cell injury.

Therefore, VC may alleviate oxidative stress in SAP via the activation of the NRF2/NQO1/HO-1 pathway. To our knowledge, this study is the first to report that VC attenuates pancreatic damage in SAP rats via an NRF2/NQO1/HO-1-mediated pathway.

There are some limitations in this study. First, this study lacks a positive control group. Second, siRNA-mediated knockdown of NRF2 is only performed *in vitro*. Further studies still need to verify the impact of knocking out this gene *in vivo* on the VC-protective effects against pancreatitis.

In conclusion, the present study shows that a high dose of VC ameliorates pancreatic injury of SAP through the NRF2/NQO1/HO-1 pathway to inhibit oxidative stress.

Acknowledgments

Funding: This work was supported by the Medical Guidance Project of Shanghai Municipal Committee of Science and Technology (18411966400) to YC, Shanghai Municipal Commission of Health and Family Planning (2016ZB0206, ZHYY-ZXYJHZX-1-201702) to EZC, and National Natural Science Foundation of China (81600501) to YC. This work was also supported by Medical Guidance Project of Shanghai Municipal Committee of Science and Technology (16411970700) to EQM.

Footnote

Reporting Checklist: The authors have completed the ARRIVE reporting checklist. Available at http://dx.doi.org/10.21037/atm-19-4552

Data Sharing Statement: Available at http://dx.doi.org/10.21037/atm-19-4552

Peer Review File: Available at http://dx.doi.org/10.21037/atm-19-4552

Conflicts of Interest: All authors have completed the ICMJE uniform disclosure form (available at http://dx.doi.org/10.21037/atm-19-4552). The authors have no conflicts of interest to declare.

Ethical Statement: The authors are accountable for all aspects of the work in ensuring that questions related to the accuracy or integrity of any part of the work are appropriately investigated and resolved. Experiments were performed under a project license {No: SYXK[SHANG HAI] 2018-0027} granted by institutional of Animal Care and Use Committee, in compliance with Chinese guidelines for the care and use of animals.

References

1. Banks PA, Bollen TL, Dervenis C, et al. Classification of acute pancreatitis--2012: revision of the Atlanta classification and definitions by international consensus. Gut 2013;62:102-11.
2. Petrov MS, Shanbhag S, Chakraborty M, et al. Organ failure and infection of pancreatic necrosis as determinants of mortality in patients with acute pancreatitis. Gastroenterology 2010;139:813-20.
3. Garg PK, Singh VP. Organ Failure Due to Systemic Injury in Acute Pancreatitis. Gastroenterology 2019;156:2008-23.
4. Lankisch PG, Apte M, Banks PA. Acute pancreatitis. Lancet 2015;386:85-96.
5. Gryshchenko O, Gerasimenko JV, Gerasimenko OV, et al. Ca(2+) signals mediated by bradykinin type 2 receptors in normal pancreatic stellate cells can be inhibited by specific Ca(2+) channel blockade. J Physiol (Lond) 2016;594:281-93.
6. Gukovskaya AS, Gukovsky I, Algül H, et al. Autophagy, Inflammation, and Immune Dysfunction in the Pathogenesis of Pancreatitis. Gastroenterology 2017;153:1212-26.
7. Jung KH, Hong SW, Zheng HM, et al. Melatonin ameliorates cerulein-induced pancreatitis by the modulation of nuclear erythroid 2-related factor 2 and nuclear factor-kappaB in rats. J Pineal Res 2010;48:239-50.
8. Tsai K, Wang SS, Chen TS, et al. Oxidative stress: an important phenomenon with pathogenetic significance in the progression of acute pancreatitis. Gut 1998;42:850-5.

9. Liu X, Zhu Q, Zhang M, et al. Isoliquiritigenin Ameliorates Acute Pancreatitis in Mice via Inhibition of Oxidative Stress and Modulation of the Nrf2/HO-1 Pathway. Oxid Med Cell Longev 2018;2018:7161592.
10. Dong Z, Shang H, Chen YQ, et al. Sulforaphane Protects Pancreatic Acinar Cell Injury by Modulating Nrf2-Mediated Oxidative Stress and NLRP3 Inflammatory Pathway. Oxid Med Cell Longev 2016;2016:7864150.
11. Cloer EW, Goldfarb D, Schrank TP, et al. NRF2 Activation in Cancer: From DNA to Protein. Cancer Res 2019;79:889-98.
12. Kobayashi A, Kang MI, Watai Y, et al. Oxidative and electrophilic stresses activate Nrf2 through inhibition of ubiquitination activity of Keap1. Mol Cell Biol 2006;26:221-9.
13. Kobayashi A, Kang MI, Okawa H, et al. Oxidative stress sensor Keap1 functions as an adaptor for Cul3-based E3 ligase to regulate proteasomal degradation of Nrf2. Mol Cell Biol 2004;24:7130-9.
14. Spoelstra-de Man AME, Elbers PWG, Oudemans-van Straaten HM. Making sense of early high-dose intravenous vitamin C in ischemia/reperfusion injury. Crit Care 2018;22:70.
15. Schorah CJ, Downing C, Piripitsi A, et al. Total vitamin C, ascorbic acid, and dehydroascorbic acid concentrations in plasma of critically ill patients. Am J Clin Nutr 1996;63:760-5.
16. Du WD, Yuan ZR, Sun J, et al. Therapeutic efficacy of high-dose vitamin C on acute pancreatitis and its potential mechanisms. World J Gastroenterol 2003;9:2565-9.
17. Marik PE. Vitamin C for the treatment of sepsis: The scientific rationale. Pharmacol Ther 2018;189:63-70.
18. Qi MZ, Yao Y, Xie RL, et al. Intravenous Vitamin C attenuates hemorrhagic shock-related renal injury through the induction of SIRT1 in rats. Biochem Biophys Res Commun 2018;501:358-64.
19. Zhao B, Fei J, Chen Y, et al. Vitamin C treatment attenuates hemorrhagic shock related multi-organ injuries through the induction of heme oxygenase-1. BMC Complement Altern Med 2014;14:442.
20. Laukkarinen JM, Van Acker GJ, Weiss ER, et al. A mouse model of acute biliary pancreatitis induced by retrograde pancreatic duct infusion of Na-taurocholate. Gut 2007;56:1590-8.
21. Van Laethem JL, Marchant A, Delvaux A, et al. Interleukin 10 prevents necrosis in murine experimental acute pancreatitis. Gastroenterology 1995;108:1917-22.
22. Kruse P, Anderson ME, Loft S. Minor role of oxidative stress during intermediate phase of acute pancreatitis in rats. Free Radic Biol Med 2001;30:309-17.
23. de Grooth HJ, Manubulu-Choo WP, Zandvliet AS, et al. Vitamin C Pharmacokinetics in Critically Ill Patients: A Randomized Trial of Four IV Regimens. Chest 2018;153:1368-77.
24. Tanaka H, Matsuda T, Miyagantani Y, et al. Reduction of resuscitation fluid volumes in severely burned patients using ascorbic acid administration: a randomized, prospective study. Arch Surg 2000;135:326-31.
25. Tyml K, Li F, Wilson JX. Septic impairment of capillary blood flow requires nicotinamide adenine dinucleotide phosphate oxidase but not nitric oxide synthase and is rapidly reversed by ascorbate through an endothelial nitric oxide synthase-dependent mechanism. Crit Care Med 2008;36:2355-62.
26. Tsai MS, Huang CH, Tsai CY, et al. Ascorbic acid mitigates the myocardial injury after cardiac arrest and electrical shock. Intensive Care Med 2011;37:2033-40.
27. Cárcamo JM, Pedraza A, Bórquez-Ojeda O, et al. Vitamin C suppresses TNF alpha-induced NF kappa B activation by inhibiting I kappa B alpha phosphorylation. Biochemistry 2002;41:12995-3002.
28. Oudemans-van Straaten HM, Spoelstra-de Man AM, de Waard MC. Vitamin C revisited. Crit Care 2014;18:460.
29. Moskowitz A, Andersen LW, Huang DT, et al. Ascorbic acid, corticosteroids, and thiamine in sepsis: a review of the biologic rationale and the present state of clinical evaluation. Crit Care 2018;22:283.
30. Satoh T, Okamoto SI, Cui J, et al. Activation of the Keap1/Nrf2 pathway for neuroprotection by electrophilic [correction of electrophillic] phase II inducers. Proc Natl Acad Sci USA 2006;103:768-73.
31. Katsumata Y, Shinmura K, Sugiura Y, et al. Endogenous prostaglandin D2 and its metabolites protect the heart against ischemia-reperfusion injury by activating Nrf2. Hypertension 2014;63:80-7.
32. Liu M, Reddy NM, Higbee EM, et al. The Nrf2 triterpenoid activator, CDDO-imidazolide, protects kidneys from ischemia-reperfusion injury in mice. Kidney Int 2014;85:134-41.
33. Kanninen K, Heikkinen R, Malm T, et al. Intrahippocampal injection of a lentiviral vector expressing Nrf2 improves spatial learning in a mouse model of Alzheimer's disease. Proc Natl Acad Sci USA

2009;106:16505-10.
34. Shin S, Wakabayashi J, Yates MS, et al. Role of Nrf2 in prevention of high-fat diet-induced obesity by synthetic triterpenoid CDDO-imidazolide. Eur J Pharmacol 2009;620:138-44.
35. Uruno A, Furusawa Y, Yagishita Y, et al. The Keap1-Nrf2 system prevents onset of diabetes mellitus. Mol Cell Biol 2013;33:2996-3010.
36. Jiang T, Huang Z, Lin Y, et al. The protective role of Nrf2 in streptozotocin-induced diabetic nephropathy. Diabetes 2010;59:850-60.

Cite this article as: Xu LL, Zhao B, Sun SL, Yu SF, Wang YM, Ji R, Yang ZT, Ma L, Yao Y, Chen Y, Sheng HQ, Chen EZ, Mao EQ. High-dose vitamin C alleviates pancreatic injury via the NRF2/NQO1/HO-1 pathway in a rat model of severe acute pancreatitis. Ann Transl Med 2020;8(14):852. doi: 10.21037/atm-19-4552

Supplementary

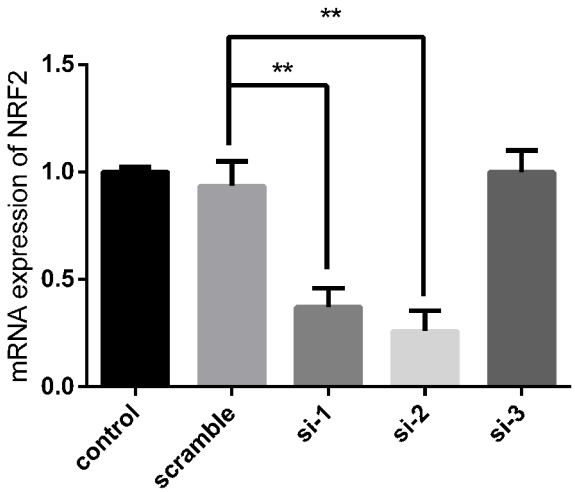

Figure S1 mRNA expression level of Nrf2 in AR42J cells after three siRNA sequence mediating knockdown of NRF2. **, P<0.01. P values were analyzed by ANOVA and unpaired Student's *t*-test. Control group, without siRNA treatment; scramble group, AR42J cells transfected with 50 nM nonspecific negative-siRNA; si-1, si-2, and si-3 group, AR42J cells transfected with three siNRF2 (50 nM), respectively; NRF2, nuclear factor erythroid-2.